RESEARCH

Open Access

Fibronectin extra domain A as a drug delivery targeting epitope for rheumatoid arthritis

Victor Z. Sun[1*] , Terry L. Melim[1], Soumya Mitra[1], Jamie E. Erickson[1], Shaughn H. Bryant[1], Avery Farnham[2], Susan Westmoreland[1], Heather Knight[1], Liang Zhang[1], Wendy Ritacco[1], Kristoff Homan[3], Lorenzo Benatuil[4], Annette J. Schwartz Sterman[1] and Andrew D. Goodearl[1]

Abstract

Objectives: To assess the ability of monoclonal antibodies (mAbs) specific for fibronectin extra-domain A (FnEDA) to target diseased tissues of mouse collagen induced arthritis (mCIA) models. To explore the parameters of the targeting exhibited by anti-FnEDA mAbs including timing and location.

Methods: Targeting capabilities of anti-FnEDA mAbs were demonstrated by biodistribution study where *i.v.* injected antibodies were detected by conjugated near-infrared (NIR) fluorophore, ^{125}I label and immunohistochemistry (IHC) of the injected antibody. Location of FnEDA expression in both mCIA and human RA tissue were mapped by IHC. Quantification of anti-FnEDA mAbs targeted to disease tissue was measured by whole-body autoradiography (WBA). Timing of the targeting was interrogated with fluorescent and confocal microscopy using anti-FnEDA mAbs labeled with different fluorophores and injected at different times.

Results: Anti-FnEDA mAbs show specific targeting to diseased paws of mCIA animal. The targeting was focused on inflamed synovium which is consistent with FnEDA expression profile in both mCIA and human RA tissues. Anti-FnEDA mAbs accumulated in diseased tissue at pharmacologically relevant concentrations, the targeting was sustained for up to 14 days and FnEDA was able to support targeting of multiple doses of anti-FnEDA mAbs given 5 days apart.

Conclusion: FnEDA is specifically upregulated in the inflamed tissues of mCIA. Antibodies specific for FnEDA can be useful as molecular delivery vehicles for disease specific targeting of payloads to inflamed joint tissue.

Introduction

Treatment of rheumatoid arthritis (RA) has greatly improved in recent decades driven in large part by biologics, most notably, biologics antagonizing TNFα. However, many treated patients only partially respond to therapy or response decreases over time leaving

significant unmet clinical needs. The advent of bispecific engineering of biologics has presented an opportunity to further develop improved therapeutics through targeted delivery [1, 2]. Selectively delivering drugs to areas affected by disease ensures optimal and prolonged exposure at the relevant site [3–5]. Combined with engineering to decrease systematic circulation, this technology platform could increase efficacy, improve dosing frequency, decrease side effects, and potentially enable delivery of payloads that might otherwise not be tolerated. Cytokines are an attractive

*Correspondence: victor.sun@abbvie.com

[1] Drug Discovery Science and Technology, Abbvie Bioresearch Center, Worcester, MA, USA
Full list of author information is available at the end of the article

Sun *et al. Advances in Rheumatology*   (2022) 62:17

Page 2 of 11

class of therapeutic agents that can benefit from the targeted approach in the form of immunocytokines. Although the antibody targeted delivery of cytokines is still in relative early stage of research and development, there is emerging clinical validation of this approach in oncology and more recently in autoimmune disease [6–8].

To achieve antibody targeted delivery of biologics, a disease specific epitope is needed. Ideally, a targeting epitope for drug delivery should have minimal expression in normal tissue, be accessible by large biologics and expressed in sufficient quantity at the diseased site to allow delivery of payloads at pharmacologically relevant concentrations. Fibronectin is a widely expressed extracellular matrix protein with important roles in cell adhesion through its interaction with integrins. Fibronectin extra-domain A (FnEDA) is a fibronectin type III repeat module that is included in the fibronectin sequence through alternative splicing in a number of disease circumstances, examples include growing tumors, development of fibrotic pathology as well as in autoimmune disease such as rheumatoid arthritis and IBD [8–10]. In human RA samples, FnEDA expression is predominantly associated with the proliferating synovial inflamed pannus tissue [11, 12], offering an excellent expression profile to support targeted immunocytokine therapy.

Antibodies targeting FnEDA, in small immunoprotein and diabody IL10 fusion formats, have been evaluated previously as vehicles for targeted delivery of biologics for the treatment of RA in the mouse collagen induced arthritis model [13]. This prior report elegantly demonstrates that the FnEDA targeted diabody is enriched in the inflamed joints of mCIA animal relative to noninflamed paws and negative control constructs. High resolution immunostaining of the diabody showed the distribution pattern to be predominantly perivascular in nature, consistent with observations of targeting in tumor neovasculature with similar constructs [7, 14, 15]. In addition, recent publication used PET imaging to show similar FnEDA targeted immunocytokine was able to concentrate in the inflamed joints of RA patients which demonstrates a successful translation from rodent to human [16]. In order to further characterize the targeting of FnEDA specific antibodies in mCIA models, we undertook biodistribution studies of anti-FnEDA antibodies and characterized targeting at the organ level with ex vivo imaging, at tissue level with high resolution immunohistochemistry and using quantitative detection methods. Having established that FnEDA targeted antibodies directly accumulate in the inflamed synovium, consistent with the human immunoreactivity profile, we proceeded to characterize other properties important to the therapeutic deployment of FnEDA targeting, including tissue retention time, dose-dependence and repeat dosing properties.

Materials and methods

Anti-FnEDA mAb generation, fluorescent labeling, and characterization

The anti-FnEDA mAbs used in this manuscript were generated at Abbvie and described previously [6]. Antibody used in human IHC were purchased (Abcam). Consistent with previous reports, the anti-FnEDA antibodies were able to specifically bind to fibronectin containing the splice insertion of EDA with no binding to plasma fibronectin that does not contain the FnEDA. To enable biodistribution studies, anti-FnEDA mAb and nonspecific control anti-Tetanus Toxoid (TeTx) mAb was conjugated to Alexa Fluor 488 (AF488), Alexa Fluor 647 (AF647) (ThermoFisher) and IRDye® 800CW (LiCor) through N-Hydroxysuccinimide ester chemistry following a modified protocol based on manufacture supplied instructions. Briefly, the antibody was buffer exchanged into PBS pH 8.0 and threefold molar excess of amine-reactive fluorescent dye was added to the antibody solution. The mixture was incubated at room temperature with gentle shaking for 2 h. Buffer exchange to PBS pH 7.4 and removal of free dye was accomplished using PD 10 desalting columns (GE Life Science). ELISA binding assay was used to evaluate specific binding to FnEDA and whether the fluorescent labeling of the mAbs affected the binding behavior. In this assay, 96-well EIA/RIA clear flat-bottom microplate (Corning) was coated with recombinant fibronectin containing EDA and plasma FN that does not contain EDA (R&D Systems) at 1 µg/mL. Next, the anti-FnEDA and anti-TeTx mAbs were serial diluted from 10 µg/mL down to 0.0006 µg/mL onto the ELISA plate. After washing, HRP-conjugated goat anti-human secondary antibody (Thermo Fisher Scientific) were added. Finally, the plate was washed again and detected with 1-step TMB substrate and quenched with equal volume of 2 N sulfuric acid (Invitrogen). The stability of labeled antibodies, and sufficient removal of free dye was checked with analytical size-exclusion chromatography (AnSEC) using Superdex 200 increase 5/150 gl column (GE Life Science). The degree of label was calculated using absorbance values of protein and dye. Uniform fluorescent intensity at same concentration was also confirmed using Odyssey CLx NIR Imaging System (LiCor).

Collagen-induced arthritis mouse model

Male DBA/1 J mice (The Jackson Laboratory) were used at 6–8 weeks of age. Mice utilized in these studies were conducted at AbbVie to the standards of the Association for the Assessment and Accreditation of Laboratory

Sun *et al. Advances in Rheumatology*　　　(2022) 62:17

Page 3 of 11

Animal Care Standards. All studies with mice were performed according to approved protocols by AbbVie's Institutional Animal Care and Use Committee (IACUC). Arthritis was induced with an intradermal injection at the base of the tail with 100 µl emulsion containing 100 µg type II bovine collagen in 0.1 N acetic acid and 100 µl complete Freund's adjuvant containing 100 µg Mycobacterium tuberculosis H37Ra (BD Difco). A boost of 1.0 mg zymosan A in 200 µl phosphate-buffered saline (Life Technologies, Grand Island, NY) was given 21 days later via an *i.p* injection. Disease onset occurred within 3–7 days following the boost, and mice were monitored daily for a change in paw swelling with a caliper thickness gauge (Dyer).

Immunohistochemical analysis of mouse and human tissue

All immunohistochemistry (IHC) was performed on the Leica Bond RX. Human RA synovium samples were evaluated for fibronectin EDA expression with a mouse anti-FnEDA monoclonal antibody (Abcam). Formalin-fixed, paraffin-embedded (FFPE) tissue was obtained from Folio Biosciences (Discovery Life Sciences Huntsville, AL, samples provided under agreement 00007398.0). Following baking and deparaffinization, tissue sections were blocked with both dual endogenous block (Agilent) and protein block (Agilent). The epitope was unmasked enzymatically with proteinase K (Agilent) prior to a 30-min incubation with the primary antibody at 7.5 ug/ml, detected with Leica's HRP polymer, and visualized with DAB (Leica's Bond Polymer Refine Detection kit) with a hematoxylin counterstain.

FFPE Mouse CIA paws, decalcified with either EDTA or Calrite, were stained with biotin-labeled human monoclonal FnEDA. Tissue sections were baked at 60 °C, deparaffinized and rehydrated through graded alcohols. The epitope was unmasked using overnight heat pretreatment at 60 °C with Leica's citrate buffer; enzymatic pretreatment with protease 1 (Roche) was also used while running IHC on the Bond platform. Tissue sections were blocked with dual endogenous block, streptavidin/biotin blocking kit (Vector Labs), and protein block prior to a 60-min incubation with the primary antibody, human FnEDA-biotin labeled at 10 µg/ml. The FnEDA was detected with Vectastain elite ABC-HRP reagent (Vector Labs) or donkey anti-human HRP conjugated secondary (Thermo) and visualized with DAB (Leica Bond Polymer Refine Detection kit) with a hematoxylin counterstain. All slides were scanned on a Pannoramic 250 Slide Scanner (3D Histech).

800CW-NIR fluorescence biodistribution

To compare the targeting of anti-FnEDA mAbs in disease vs. normal tissues, mCIA animals were enrolled between days 24 and 28 at the first clinical signs of disease and were used for imaging at peak inflammation on day 7 post-enrollment.

Conjugation of anti-FnEDA antibody with IRDye 800CW-NHS ester (Li-COR) was performed according to methods described in a previous section. For organ distribution, 5 mg/kg of labeled anti-FnEDA and anti-TeTx were administered through an *i.v.* injection to mCIA and naïve mice, 3 mice per group. Injected mice were euthanized at 72 h post-administration, perfused with saline and the organs were excised to acquire fluorescence images across different tissues using a LiCOR Pearl imaging system. Mean fluorescence was determined from using ImageStudio software (Li-COR) by subtracting the background, drawing a region of interest around the organs, and using a measure function to determine the mean value.

Targeting of a single-dose anti-FnEDA mAb to inflamed joints

To assess the ability of anti-FnEDA mAb to target and be retained in the inflamed joints, naïve and mCIA mice received 5 mg/kg of anti-FnEDA or anti-TeTx mAb through *i.v.* injections on day 31 after disease induction. Animals were euthanized 48 h after administration of the antibodies and tissues were harvested and processed by FFPE and sectioned to 5 µm, followed by immunohistochemical detection of the injected human antibody.

To investigate antibody retention in the diseased tissues, 9 naïve and 9 mCIA mice received 5 mg/kg of anti-FnEDA mAb *i.v.* injections on day 31 after disease induction. Three animals were euthanized at each time point 48 h, 6 days or 13 days following administration of the mAb. Tissues were processed by FFPE and sectioned, followed by immunohistochemistry to detect the human mAb.

To understand the targeting performance of the anti-FnEDA antibody at different doses, 3 mCIA mice each group were administered through *i.v.* injections with 3, 1, 0.3 and 0.1 mg/kg of anti-FnEDA antibody on day 31 after disease induction. Animals were euthanized after 48 h, and FFPE sections of collected tissue were analyzed with anti-human IHC detection.

Whole-body autoradiography (WBA)
Reagents

The Anti-FnEDA mAb and anti-TeTx Antibodies were labeled with ^{125}I through PerkinElmer Life and Analytical Sciences via a modified lactoperoxidase procedure with BSA carrier was added to retard radiolysis. The iodinated antibodies were to be more than 95% pure with specific activity of 10.1uCi/ug.

Whole-body tissue preparation study 1.

Sun *et al. Advances in Rheumatology*   (2022) 62:17

Page 4 of 11

Ten CIA mice each group were dosed *i.v.* with 5mpk cold Anti-FnEDA or anti-TeTx and (80uCi/Kg) ^{125}I labeled Anti-FnEDA or anti-TeTx and euthanized 48 h. after injection. Mice were frozen over hexane/dry ice for 30 min, dried off and placed in − 80 ℃ overnight. The frozen mice were casted in blocks of 3% carboxymethyllcellulose (CMC). Cryosectioning was performed with a Leica CM 3600 to collected 40 μm sections at 3 levels of interest in the sagittal plane so that all major tissues, organs, and biological fluids were included. Representative sections were freeze-dried at −20 ℃ and mounted onto cardboard wrapped with Mylar film and exposed on phosphorimaging screens along with autoradiographic standards. The autoradiographic standards and image data were sampled using MCID software to create a calibrated standard curve to convert nanocuries/g to ng equivalents/g.

Mouse paw autoradiography study 2
CIA mice were dosed IV with 5mpk cold anti-FnEDA or anti-TeTx and (80uCi/Kg) ^{125}I labeled Anti-FnEDA or anti-TeTx. Based on blood radioactive levels, 14-day time point was chosen to allow the systemic clearance of dosed antibodies. All mice were euthanized by asphyxiation on day 14 after injection. The paws were dissected and fixed in formalin for 24 h, decalcified, infiltrated with sucrose, and embedded in OCT, sectioned at 40 μm and mounted onto glass slides.

The radioactive blood standards were prepared by spiking radiolabeled antibodies into blood and serially diluted over the desired concentration range of 0.0024 to 5 uCi/ml. Multiple holes were drilled into a CMC block which was filled with standards processed similarly to CMC blocks with paws.

Dual injection study
The anti-FnEDA mAb labeled with AF488 or AF594 were tested to ensure binding was not affected by the attached fluorophore (data not shown). The mCIA mice 31 days after disease induction were first injected 5 mg/kg of Anti-FnEDA-AF488, and a second dose of anti-FnEDA-AF594 was administered also at 5 mg/kg 5 days later to simulate 2x/week dosing regimen. On the 7th day after first injection, animals were euthanized, and inflamed joints were harvested and embedded into fresh frozen OCT blocks. Sections of the inflamed joints were imaged using a Nuance Spectral imaging camera (Perkin Elmer). SP5 Laser Scanning Confocal Microscope (Leica) was used as orthogonal confirmation of florescent signal from dual injections. Sequential scans were performed with excitation with 405 nm and 594 nm lasers for the first scan and 488 nm laser in second scan. Emission spectrum collection was done with hybrid detector,

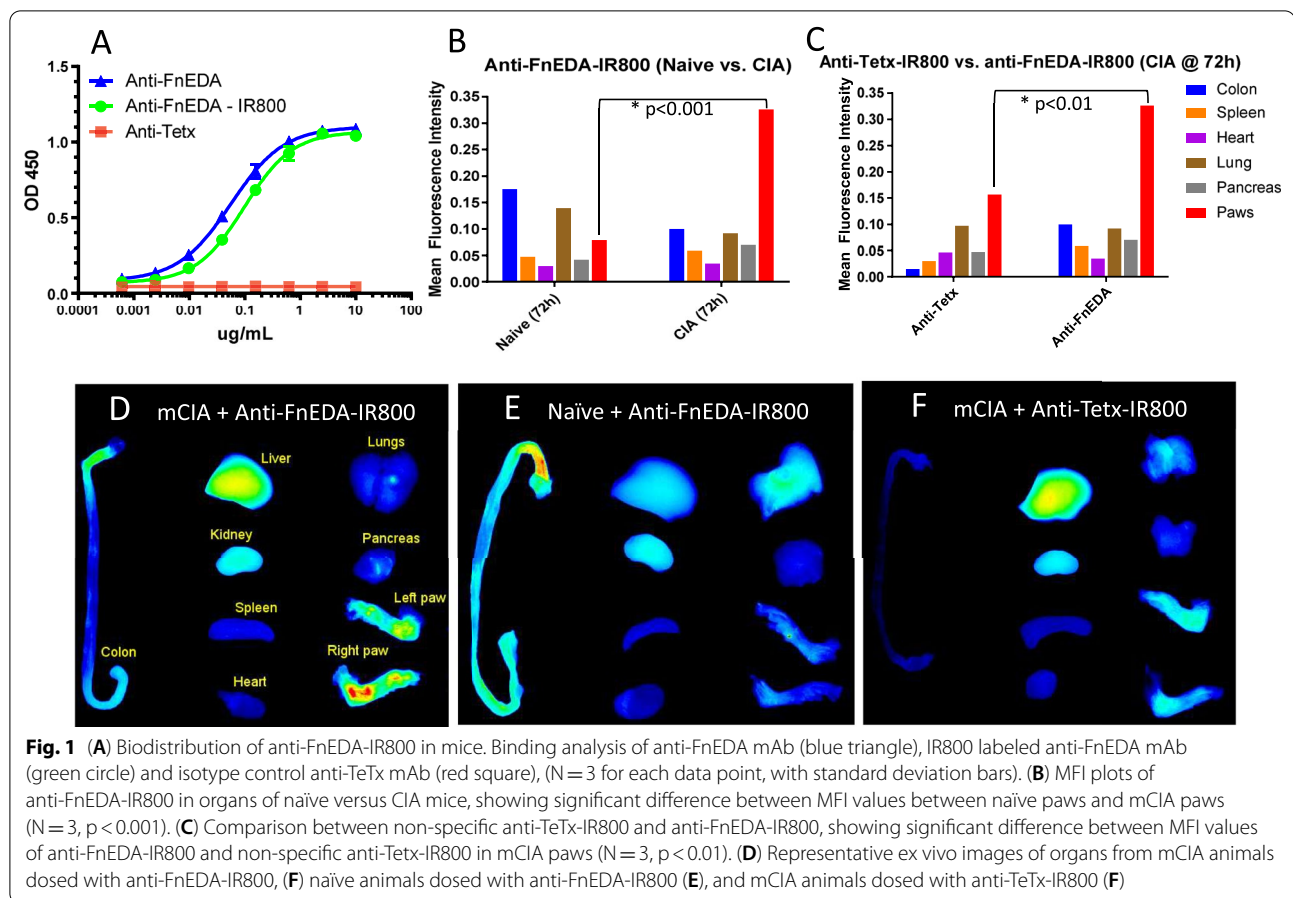bandwidths were adjusted with Acousto Optic Tunable Filters to avoid signal bleed through of different channels.

Results
Evaluation of disease specific tissue targeting using NIR-labeled anti-FnEDA antibody
To evaluate the disease tissue-targeting ability of anti-FnEDA mAb in vivo and assess nonspecific tissue binding, tissue biodistribution studies were conducted using NIR optical imaging with 800CW-labeled antibodies in whole mount organ samples. The labeled antibodies were extensively characterized and found to have a degree of labeled between 1.5 to 2 dye molecules per antibody, no aggregation detected by AnSEC (data not shown), and no change in binding capability to FnEDA (Fig. 1A). Figure 1 summarizes the imaging data obtained using anti-FnEDA and the anti-TeTx control antibody after a single 5 mg/kg *i.v.* injection. As shown, analysis of tissues collected from naïve and CIA animals dosed with anti-FnEDA mAb revealed that the 800CW mean signals in paws of CIA mice (0.3 ± 0.1) were markedly higher (p < 0.001) than those in naïve paws (0.08 ± 0.01) (Fig. 1B). The biodistribution profiles (Fig. 1C) showed that when compared with anti-TeTx control, significantly more anti-FnEDA mAb was retained in the inflamed paw (p < 0.01), indicating epitope-specific targeting. All the other organs displayed comparable uptake for both the antibodies. The data for kidney and liver were not enumerated as they are the clearance organs with very high non-specific signals. Representative fluorescent images of the organs from the study are shown (Fig. 1D–F).

Anti-human IHC detection after single dose i.v. injection of anti-FnEDA antibody
In addition to NIR imaging, which quantitates relative levels of injected antibody in different organs, IHC was also used to provide high resolution insight into the location of antibody distribution within a tissue. Looking at the distribution of unlabeled antibodies is also a check to ensure fluorescent labeling did not alter the distribution behavior of antibody within the body. Imaging of inflamed knee joints showed that systemically administered anti-FnEDA antibody associated with disease-related tissue features with high levels of specificity. Intense immunoreactivity is observed in the inflamed synovium (Fig. 2A, C) and focal erosion pits in the knee (Fig. 2B). Levels of anti-FnEDA in representative soft tissue organs of mCIA animal was much lower (Fig. 2D–F). The non-specific anti-TeTx mAb showed minimal levels in the inflamed knee joint of mCIA animal (Fig. 2G). While biodistribution studies were generally conducted at 2- or 3-day time points, single injection of anti-FnEDA

Fig. 1 (**A**) Biodistribution of anti-FnEDA-IR800 in mice. Binding analysis of anti-FnEDA mAb (blue triangle), IR800 labeled anti-FnEDA mAb (green circle) and isotype control anti-TeTx mAb (red square), (N = 3 for each data point, with standard deviation bars). (**B**) MFI plots of anti-FnEDA-IR800 in organs of naïve versus CIA mice, showing significant difference between MFI values between naïve paws and mCIA paws (N = 3, p < 0.001). (**C**) Comparison between non-specific anti-TeTx-IR800 and anti-FnEDA-IR800, showing significant difference between MFI values of anti-FnEDA-IR800 and non-specific anti-Tetx-IR800 in mCIA paws (N = 3, p < 0.01). (**D**) Representative ex vivo images of organs from mCIA animals dosed with anti-FnEDA-IR800, (**F**) naïve animals dosed with anti-FnEDA-IR800 (**E**), and mCIA animals dosed with anti-TeTx-IR800 (**F**)

mAb at 5 mg/kg was still detectable in the inflamed knee joints after 6 days and 13 days (Fig. 3C, D).

In a parallel experiment, the dose–response of anti-FnEDA antibody in tissue targeting was evaluated. The anti-FnEDA mAb was administered at concentrations of 3, 1, 0.3 or 0.1 mg/kg into mCIA animals and the inflamed knee joints were analyzed by anti-human IHC detection. As shown, the labeling intensity of anti-FnEDA mAb administered at 3 mg/kg (Fig. 3E) was nearly equal to that seen in previous studies at 5 mg/kg (Fig. 3B). Lower doses showed less intense tissue targeting by the anti-FnEDA antibody (Fig. 3F–H). The two lowest doses also showed less comprehensive targeting to the inflamed areas within the joint. Anti-FnEDA mAb dosed into naïve mice did not show any detectable distribution into the joints (Fig. 3A).

FnEDA expression in human and mouse inflamed joints

The biodistribution data show that anti-FnEDA mAb was able to target the inflamed synovium in mCIA knee joints. However, contrary to previous literature reports, very little retention in the perivascular space was observed. To ascertain the biodistribution data

matches the FnEDA expression profile in RA, IHC analysis was performed on both mCIA and human RA tissues. In mCIA ankles, IHC confirmed robust expression of FnEDA in the inflamed synovium (Fig. 4A, C), while higher resolution images show staining around vessels is less consistent and slightly less pronounced (Fig. 4B, D). FnEDA was detected in human RA tissue primarily in the lining synovial fibroblasts with little to no staining in sublining fibroblasts or around vessels (Fig. 4E, F). The IHC expression data therefore suggests that the lack of observation of perivascular uptake with dosed anti-FnEDA mAb in the biodistribution studies is either due to the signal sensitivity from antibody associated with the vascular regions or clearance of the antibody at time-points of 48 h or later.

Whole-body autoradiography

Thus far, NIR biodistribution and IHC images show systemically administered anti-FnEDA antibody was able to concentrate in the disease area more than control tissue, which is an important characteristic for an antibody to be used as a drug delivery vehicle. Another important characteristic is the sustained level of antibody
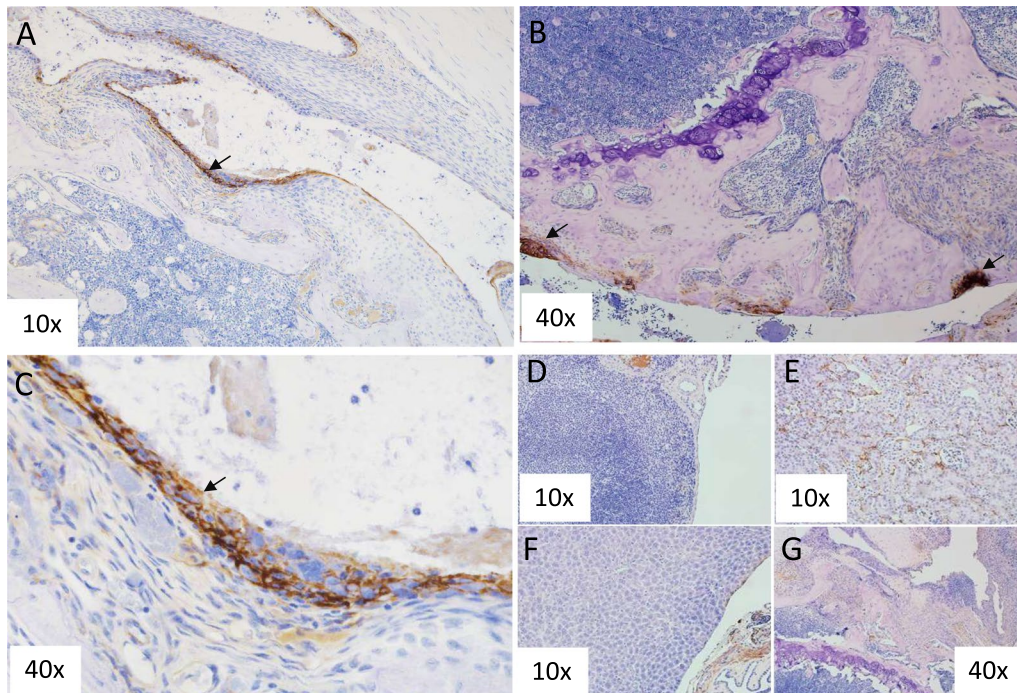
Fig. 2 Anti-FnEDA mAb biodistribution detected by anti-human IHC. Biodistribution into inflamed knee joints (**A**–**C**), contrasts with non-specific organs shown in spleen (**D**), kidney (**E**) and liver (**F**); inflamed joints from animal treated with isotype control anti-TeTx antibody (**G**). Arrows point to disease specific structures (N = 3, Arrows in **A** and **C** point to inflamed synovium, arrows in **B** indicates focal erosion pits, magnification level is noted in each picture)
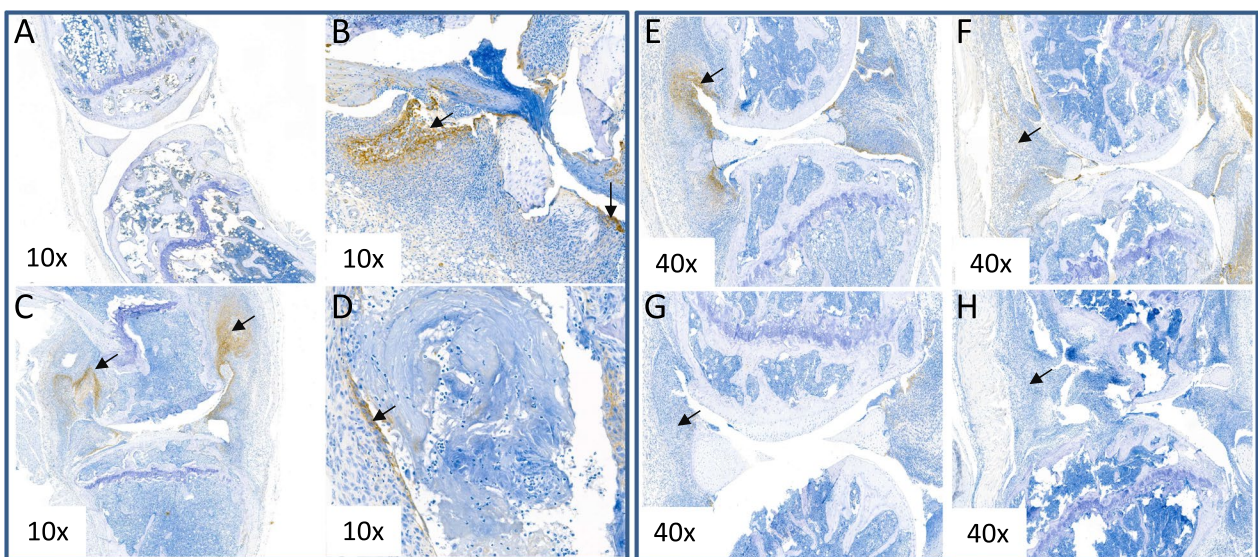

Fig. 3 Duration and dose-down of anti-FnEDA biodistribution in mCIA joint tissue. Dosed anti-FnEDA mAb detected by IHC in joints of naïve animal (**A**) and mCIA animal after 48 h (**B**), 6 days (**C**) and 13 days (**D**). For dose-down study, i.v. injection was administered to mCIA animals at: 3 mg/kg (**E**), 1 mg/kg (**F**), 0.3 mg/kg (**G**) and 0.1 mg/kg (**H**). (N = 3, Arrows point to disease specific structures, magnification level is noted in each picture)

Sun *et al. Advances in Rheumatology*   (2022) 62:17

Page 7 of 11
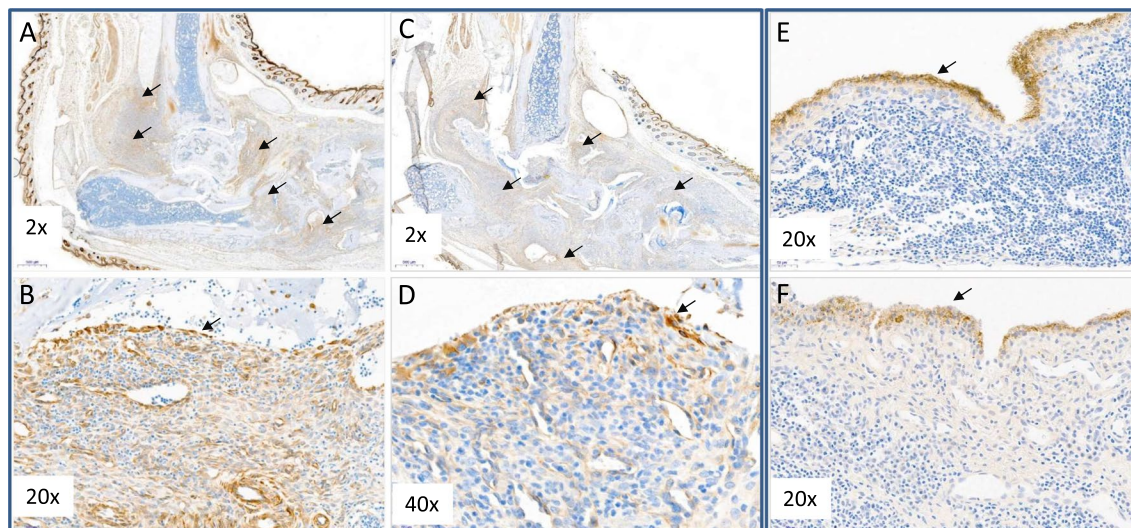
Fig. 4 Immunohistochemistry detection for FnEDA epitope. mCIA ankle(**A**–**D**) and human RA tissue (**E**, **F**) sections were labeled with anti-FnEDA mAb and detected with HRP-labeled secondary mAb (brown). (N = 3, Arrows points to areas of inflammation, magnification level is noted in each picture)

that reached the diseased area, as this parameter will be helpful in choosing viable payload pairings. In order to quantify the levels of targeted antibody, whole body autoradiography (WBA) experiments were performed to quantify the concentration of ^{125}I-anti-FnEDA and ^{125}I-anti-TeTx antibodies in the inflamed paw. Consistent with NIR biodistribution and IHC data, the whole-body image (Fig. 5A) showed much higher levels anti-FnEDA antibody in the inflamed knee and paw compared with anti-TeTx antibody. To confirm the radioactive signal did not come from free isotope that has become detached from labeled antibody or from degraded antibody fragments, serial sections of a mCIA knee joint were collected and analyzed by IHC to compare with the WBA image (Fig. 5B). Overlay of the IHC and WBA images showed consistent co-localization of anti-FnEDA antibody and the radioactive signal, which suggests that the radiolabel was still attached to functional antibodies. The ^{125}I-anti-FnEDA consistently showed higher level of distribution into inflamed knee joints and paw compared with ^{125}I-anti-TeTx (Fig. 5C, two representative images from ten animals). The radioactive signal from selected regions (Fig. 5D) were quantified and converted to ng of antibody/g of tissue using a standard curve (Fig. 5E). This quantitative methodology demonstrates significantly greater enrichment of anti-FnEDA mAb relative to control antibody in the selected regions analyzed (p < 0.001). The observed concentration equates to around 0.1 nM at 14 days after a single dose of anti-FnEDA mAb which is more than sevenfold higher than observed concentration of anti-TeTx control antibody under similar conditions.

Dual injection study

In addition to specificity and bioavailability, an ideal epitope for targeted drug delivery should also be present in relative abundance. Abundant expression ensures that the targeting epitope will not be saturated too quickly to allow accumulation of therapeutically relevant concentration at the diseased site; it can also help sustain multiple dosing which is critical for effective treatment of chronic diseases. To check the durability of FnEDA as a targeting epitope, an experiment was performed where the same group of mCIA animals were dosed with a 5mpk dose of AF-488 labeled anti-FnEDA antibody on day 1, then a second dose of AF-594 labeled anti-FnEDA antibody was given on day 5 (Fig. 6). The day 5 time point for the second dose was chosen to simulate twice a week dosing regimen with the imaging time point at 7 days from first dose, which is well within the retention time window of anti-FnEDA mAbs in inflamed joints as suggested by the WBA study. Microscopy images clearly show significant labeling of the inflamed pannus tissue with both fluorophores, indicating that the first dose of anti-FnEDA-AF488 at 5 mg/kg did not stop the second dose of anti-FnEDA-AF594 from targeting similar regions in the inflamed joint. In some sections, the fluorescent pattern of the two doses was significantly overlapping, giving a yellow appearance to the image (Fig. 6C, D). In other sections, more separated labeling patterns were observed (Fig. 6A, B), and most of the anti-FnEDA mAb distributed to areas with structural features of pannus, consistent with IHC, WBA and NIR imaging methodologies. Although there are signals associated with blood vessels

Fig. 5 Whole body autoradiography in mCIA model. Comparison of mCIA mice dosed with ^{125}I labeled anti-FnEDA (left) and control ^{125}I labeled anti-TeTx mAb (right) (**A**). IHC detection of anti-FnEDA mAbs overlaid with the radio signal (**B**). Representative paws from animals dosed with Anti-FnEDA or Anti-TeTx (**C**). For each paw, 3 circles with identical area were drawn over high intensity areas (**D**), and the radioactive signal from these circles were converted to amount of antibody based on a standard curve and plotted (**E**). (Red bar represents the average amount of antibody extrapolated from such areas in joints of mice treated with anti-FnEDA mAb with standard deviation, N = 9. Blue bar represents the average amount of antibody extrapolated from such areas in joints of mice treated with anti-TeTx mAb with standard deviation, N = 9.)

(Fig. 6C), it is worth noting that these signals are predominantly from the second dose of anti-FnEDA-AF594. This could be due to the fact that 48 h between the second dose and imaging time was insufficient for blood clearance.

Discussion

In this study, we have confirmed and demonstrated with four different detection methods that the anti-FnEDA antibodies are able to target and concentrate in the inflamed joints of diseased animals in the CIA model significantly better than a non-specific control antibody. Using radiolabeled antibody, we have observed a close correspondence with inflamed pathology and at high resolution have observed targeting of the synovial pannus, a major site of inflammation and mediator of disease mechanisms. This observation is consistent with the expression pattern of fibronectin detected in human rheumatoid arthritis tissue and thus validates the mouse CIA model as a translationally relevant model to characterize the targeting properties of therapeutics intended for human use [11, 12]. Although the upregulation of FnEDA in the inflamed synovium has been indirectly suggested in previous studies[17], current study offer

histological proof that this upregulation is specifically associated with areas of tissue that demonstrate disease pathology. The efficient targeting of anti-FnEDA antibody to the pannus and other disease-associated inflamed structures in Fig. 2 helps explain the observed efficacy of FnEDA targeted anti-inflammatory immunocytokines such as IL10 [13] and IL4 [18]. In contrast to these previous studies, we only observed occasional targeting to perivascular tissue. The reason for such differences is unclear but could include differences in the timing of dosing, timing of tissue harvesting, methodological differences in antibody detection and/or format/epitope differences in the FnEDA test articles deployed.

In addition to confirming distribution of anti-FnEDA antibody to the arthritic joints, the current study also evaluated various parameters that would be important in designing effective targeted delivery strategies. We find that a single dose of anti-FnEDA antibody was observable in the disease tissue for up to two weeks (Fig. 3D). This is likely a product of high tissue retention rather than sustained targeting by circulating antibodies since the measured half-life of the anti-FnEDA antibody was 5–6 days (data not shown). Targeting to inflamed pannus was observed at doses between 0.1 and 5 mg/kg, a dose range
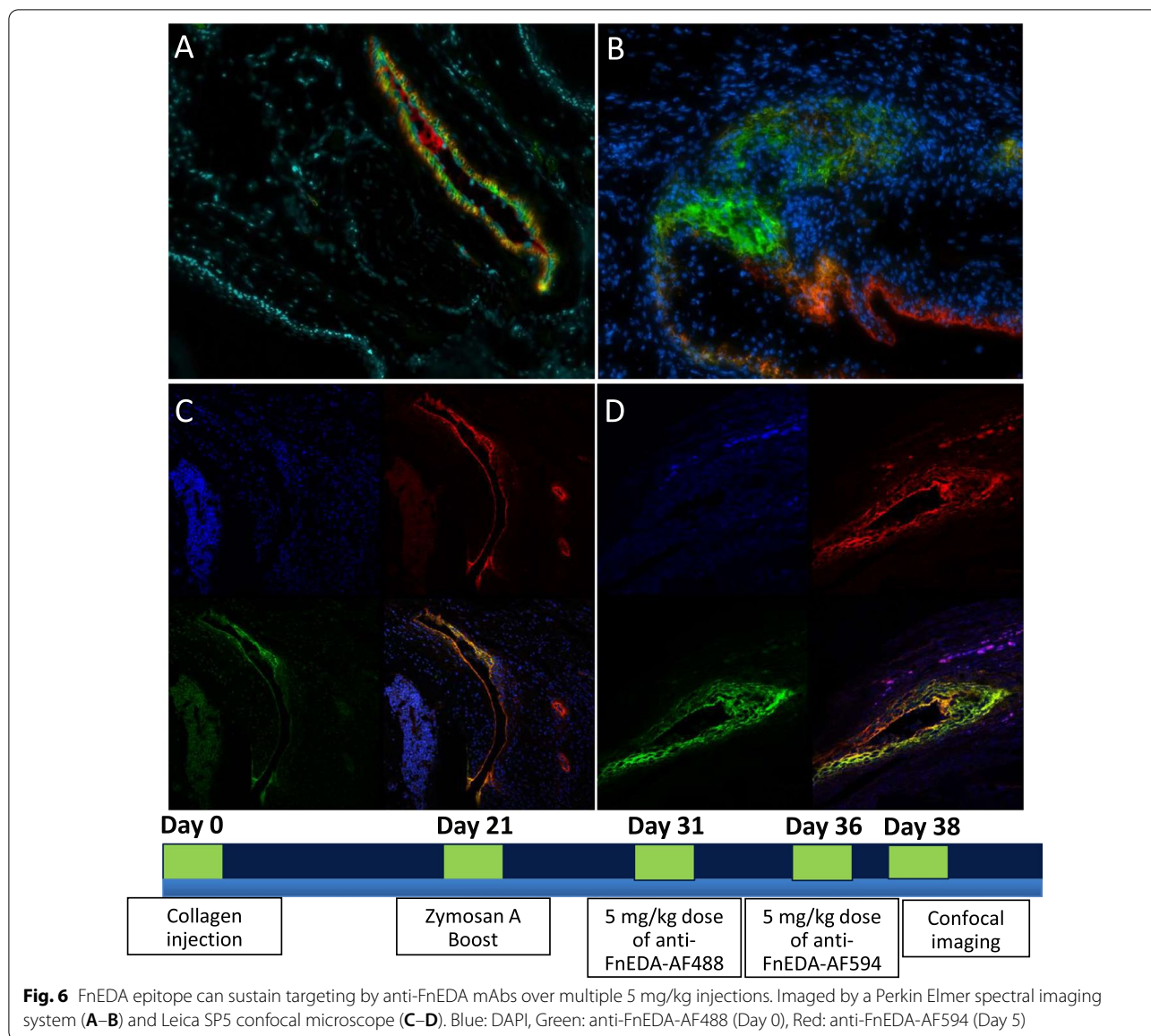
Fig. 6 FnEDA epitope can sustain targeting by anti-FnEDA mAbs over multiple 5 mg/kg injections. Imaged by a Perkin Elmer spectral imaging system (**A**–**B**) and Leica SP5 confocal microscope (**C**–**D**). Blue: DAPI, Green: anti-FnEDA-AF488 (Day 0), Red: anti-FnEDA-AF594 (Day 5)

that is highly relevant to human therapy. We also find that the FnEDA in the inflamed joints could sustain multiple doses of the targeting antibody, another important feature of a targeting epitope for human therapy. While both doses targeted inflamed synovial tissue, there was some diversity observed in the relative distribution of the two doses in this study, ranging from complete overlap of the two dosed antibodies to separate patches of labeling. Further investigations will be needed to determine whether this is due to sub-saturating dose of the antibody, dissociation of first dose bound antibody or due to synthesis and deposition of new FnEDA between doses.

FnEDA targeting of therapeutics has been extensively studied in the context of cancer therapeutic immunocytokines [19]. In in vivo animal studies, there is strong evidence for the FnEDA epitope to be predominantly perivascular in nature [15, 18]. Our observations confirm the existence of targeting of FnEDA antibodies to the perivascular space of some blood vessels in inflamed tissue. However, the signal is weak compared with the labeling of the inflamed pannus tissue. Thus, induction of FnEDA expression is not just associated with new blood vessels but is directly associated with the inflammatory tissue itself, consistent with reports of synthesis by inflammatory synoviocytes in the diseased joints [12, 20].

In this study, we have focused on the targeting of anti-FnEDA antibodies to the inflamed synovium in the mouse CIA model with a pattern that is consistent with

Sun *et al. Advances in Rheumatology* (2022) 62:17

Page 10 of 11

the observed expression of FnEDA protein in human rheumatoid arthritis [12]. This phenomenon may also have relevance more broadly as FnEDA expression has also been observed in human osteoarthritis samples [20]. Kragstrup et al. elegantly demonstrate the association of FnEDA staining with inflamed tissue in OA joints by immunohistochemistry and immunofluorescence methods. Thus, FnEDA targeted therapeutics with anti-inflammatory payloads may also be suitable for treating osteoarthritis patients. The elevated FnEDA expression in the inflamed synovium and focal erosion pits also makes it attractive for delivering anti-inflammatory and regenerative payloads in RA.

Conclusion

In summary, in this study we have performed a detailed characterization of the targeting performance of FnEDA specific antibodies and demonstrated the suitability of the FnEDA epitope to support targeted therapeutics in rheumatoid arthritis. FnEDA antibodies target selectively to the disease tissue, they bind immediately proximal to the pannus, the site of active inflammatory disease mechanisms, targeting is dose dependent and is sustained over multiple weeks. These studies, together with the comparable tissue expression pattern observed in human RA tissue, support the use of the mCIA model to characterize FnEDA targeted therapeutics and support their translation in the treatment of rheumatoid arthritis patients.

Author details
[1]Drug Discovery Science and Technology, Abbvie Bioresearch Center, Worcester, MA, USA. [2]Generate Biomedicines, Cambridge, MA, USA. [3]Bristol Myers Squibb, Boston, MA, USA. [4]Dragonfly Therapeutics Inc, Waltham, MA, USA.

References
1. Bahrami B, et al. Nanoparticles and targeted drug delivery in cancer therapy. Immunol Lett. 2017;190:64–83.
2. Trinh TL, et al. A synthetic aptamer-drug adduct for targeted liver cancer therapy. PLoS ONE. 2015;10(11): e0136673.
3. Dolman ME, et al. Drug targeting to the kidney: advances in the active targeting of therapeutics to proximal tubular cells. Adv Drug Deliv Rev. 2010;62(14):1344–57.
4. Liu Q, et al. Targeted drug delivery to melanoma. Adv Drug Deliv Rev. 2018;127:208–21.
5. Philip AK, Philip B. Colon targeted drug delivery systems: a review on primary and novel approaches. Oman Med J. 2010;25(2):79–87.
6. McGaraughty S, et al. Targeting anti-TGF-beta therapy to fibrotic kidneys with a dual specificity antibody approach. J Am Soc Nephrol. 2017;28(12):3616–26.
7. Schmid AS, et al. Antibody-based targeted delivery of interleukin-4 synergizes with dexamethasone for the reduction of inflammation in arthritis. Rheumatology (Oxford). 2018;57(4):748–55.
8. Schmid AS, Neri D. Advances in antibody engineering for rheumatic diseases. Nat Rev Rheumatol. 2019;15(4):197–207.
9. Zollinger AJ, Smith ML. Fibronectin, the extracellular glue. Matrix Biol. 2017;60–61:27–37.
10. Romberger DJ. Fibronectin. Int J Biochem Cell Biol. 1997;29(7):939–43.
11. Kriegsmann J, et al. Expression of fibronectin splice variants and oncofetal glycosylated fibronectin in the synovial membranes of patients with rheumatoid arthritis and osteoarthritis. Rheumatol Int. 2004;24(1):25–33.
12. Hino K, et al. EDA-containing fibronectin is synthesized from rheumatoid synovial fibroblast-like cells. Arthritis Rheum. 1995;38(5):678–83.
13. Schwager K, et al. Preclinical characterization of DEKAVIL (F8-IL10), a novel clinical-stage immunocytokine which inhibits the progression of collagen-induced arthritis. Arthritis Res Ther. 2009;11(5):R142.
14. Rybak JN, et al. The extra-domain A of fibronectin is a vascular marker of solid tumors and metastases. Cancer Res. 2007;67(22):10948–57.

15. Borsi L, et al. Selective targeting of tumoral vasculature: comparison of different formats of an antibody (L19) to the ED-B domain of fibronectin. Int J Cancer. 2002;102(1):75–85.
16. Bruijnen STG, et al. F8-IL10: a new potential antirheumatic drug evaluated by a PET-guided translational approach. Mol Pharm. 2019;16(1):273–81.
17. Przybysz M, Borysewicz K, Katnik-Prastowska I. Differences between the early and advanced stages of rheumatoid arthritis in the expression of EDA-containing fibronectin. Rheumatol Int. 2009;29(12):1397–401.
18. Hemmerle T, Doll F, Neri D. Antibody-based delivery of IL4 to the neovasculature cures mice with arthritis. Proc Natl Acad Sci U S A. 2014;111(33):12008–12.
19. Pasche N, Neri D. Immunocytokines: a novel class of potent armed antibodies. Drug Discov Today. 2012;17(11–12):583–90.
20. Kragstrup TW, et al. Fibroblast-like synovial cell production of extra domain A fibronectin associates with inflammation in osteoarthritis. BMC Rheumatol. 2019;3:46.

Publisher's Note